Int. J. Plant Sci. 168(8):1127–1139. 2007.

1058-5893/2007/16808-0002$15.00 DOI: 10.1086/520726

HYDRAULIC CONSEQUENCES OF VESSEL EVOLUTION IN ANGIOSPERMS

J. S. Sperry,[1,*] U. G. Hacke,† T. S. Feild,‡ Y. Sano,§ and E. H. Sikkema*

*Department of Biology, University of Utah, 257S 1400E, Salt Lake City, Utah 84112, U.S.A.; †Department of Renewable Resources, University of Alberta, Edmonton, Alberta T6G 2H1, Canada; ‡Department of Ecology and Evolutionary Biology, University of Tennessee, Knoxville, Tennessee 37996, U.S.A.; and §Laboratory of Woody Plant Biology, Graduate School of Agriculture, Hokkaido University, Sapporo 060-8589, Japan

We tested two hypotheses for how vessel evolution in angiosperms influenced xylem function. First, the transition to vessels decreased resistance to flow—often considered the driving force for their evolution. Second, the transition to vessels compromised safety from cavitation—a constraint emerging from the "pit area hypothesis" for vulnerability to cavitation. Data were obtained from branch wood of 17 basal taxa with vessels and two eudicots possessing "primitive" perforation plates. Results were compared with previous data from vesselless angiosperms and eudicots with simple perforation plates. Contrary to the first hypothesis, basal taxa did not have significantly lower sapwood-specific resistivity than vesselless angiosperms, despite vessels being wider than tracheids. Eudicot resistivity was ca. 4.5 times lower. On a vessel-area basis, resistivity of "primitive" vessels (435 ± 104 MPa s m^{-2}) was lower than angiosperm tracheids (906 ± 89 MPa s m^{-2}) but still greater than eudicot vessels (91 ± 9 MPa s m^{-2}). High resistivity of primitive vessels could be attributed to their being shorter per diameter than eudicots and to high perforation plate resistivity (57% ± 15% of total) in the species with scalariform plates. In support of the second hypothesis, primitive vessels had a cavitation pressure 1.4 MPa more vulnerable than angiosperm tracheids. This "vulnerability bottleneck" may have been even more extreme without a shift in vessels to less porous interconduit pit membranes. Vessel evolution was not driven by lower flow resistance, and it may have been limited to wet habitats by cavitation risk. A subtle, context-dependent advantage to primitive vessels is consistent with the distribution of the vesselless condition in the angiosperm tree. The results imply that truly efficient and safe vessels evolved much later than vessels per se, perhaps in concordance with larger radiations among core angiosperms.

Keywords: basal angiosperm physiology, ecological wood anatomy, vessel, water transport, xylem cavitation, xylem evolution.

Introduction

The anatomy of the tracheid-to-vessel transition in angiosperms has been well studied as a result of the persistence of apparently intermediate stages in basal taxa. The transition begins with scalariform pitting in tracheid endwalls giving way to scalariform perforations in early vessel members. The trend continues with vessel members becoming shorter and wider and their scalariform plates becoming less steep and having wider openings, eventually evolving to simple plates with a single opening (Bailey and Tupper 1918; Frost 1930; Bailey 1944, 1953; Carlquist 1983, 1987, 1990, 1992*a*, 1992*c*, 1992*d*; Feild et al. 2000; Carlquist and Schneider 2002*a*). It has long been assumed that this phylogenetic and morphologic gradient was driven by selection for lower flow resistance (Carlquist 1975; Zimmermann 1983; Baas 1986). However, we know very little about the functional properties of the transitional stages in vessel evolution. Do woods with "primitive" vessels have lower flow resistance than vesselless woods? Can they be as safe from xylem cavitation as their vesselless counterparts with the increase in conduit length and width that vessel evolution entails?

[1] Author for correspondence; e-mail j.sperry@utah.edu.

Manuscript received December 2006; revised manuscript received April 2007.

We addressed these questions with a survey of wood hydraulic function across an anatomically and phylogenetically diverse sample of basal angiosperm taxa. Results are compared with vesselless angiosperms described in a companion article (Hacke et al. 2007) and with a previous survey of vessel-bearing eudicot species with simple perforation plates (Hacke et al. 2006; Sperry et al. 2006). Phylogenetic status was assessed from recent molecular phylogenies (Soltis and Soltis 2004). Most of the sampled basal study species (fig. 1; table 1) have rather primitive vessel morphology, with long scalariform perforation plates, often with pit membrane remnants (Carlquist 1990, 1992*a*, 1992*b*, 1992*d*; Carlquist and Schneider 2002*b*). Some species, however, have simple perforation plates despite their basal position. As Carlquist has emphasized, vascular evolution has evidently proceeded at a very irregular pace in different lineages (Carlquist 1992*a*, 1999). Thus, there are simple perforation plates in *Schisandra glabra* near the base of the angiosperm phylogeny, and there are long perforation plates with narrowly spaced bars in rather derived eudicots such as *Ticodendron incognitum* (Carlquist 1991, 1992*a*). Although we focus on basal taxa in this article, we have also included a few derived taxa such as *T. incognitum* with rather primitive scalariform perforation plates (fig. 1) for comparison.

The literature on vessel evolution suggests the hypothesis that vessel-bearing wood has lower flow resistance per unit

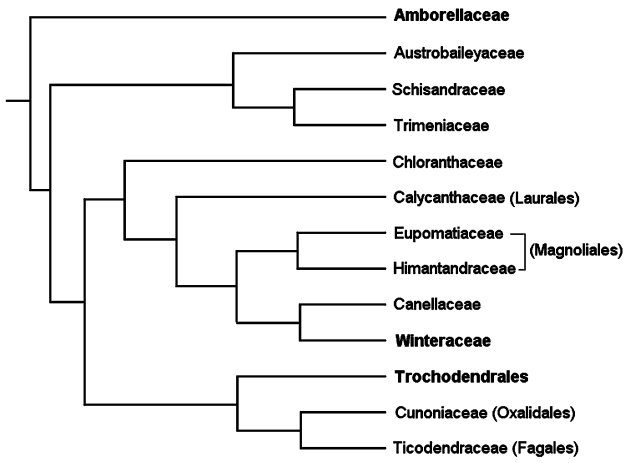

Fig. 1 Evolutionary relationships of families sampled, including those from the accompanying vesselless survey (in bold; Hacke et al. 2007). There is no significance to branch lengths. Only sampled families are shown (from Soltis and Soltis 2004).

length and per cross-sectional area (area-specific resistivity) than vesselless wood. To test this hypothesis, it is especially important to compare flow resistances between vesselless taxa and taxa with transitional vessel elements that have primitive perforation plate morphology. Long scalariform perforation plates with many bars and pit membrane remnants are an obvious factor that could minimize the advantage of "primitive" vessels relative to tracheids (Carlquist 1992*a*).

In addition to perforation plate morphology, vessel length is another factor that is crucial to flow resistance. Vessel length influences the contribution of vessel ends to the overall resistance per unit length (= resistivity) of the xylem. The shorter a vessel is for its diameter, the closer together the endwalls are, and the greater their impact on total resistivity. In eudicots, vessel length increased with diameter so as to maintain an approximately constant 56% ± 2% contribution of endwalls to the total resistivity (Hacke et al. 2006; Sperry et al. 2006). If primitive vessels are shorter for their diameter than derived vessels, they will also have greater resistivity per diameter.

A final factor compromising the conducting advantage of vessels is the area-specific resistance of their endwall pits. Interconduit pit resistance averaged 21 times higher in eudicot vessels (336 ± 81 MPa s m^{-1}; Hacke et al. 2006) than in the intertracheid pits of vesselless angiosperms (16 ± 2 MPa s m^{-1}; Hacke et al. 2007). The lower intertracheid pit resistance of vesselless angiosperms makes their woods surprisingly efficient despite the short length of tracheids (Hacke et al. 2007). Intervessel pits may have to be less porous on average than intertracheid pits to minimize the threat of cavitation by air-seeding in a larger conduit. All of these factors—perforation plate morphology, length-diameter allometry, and interconduit pitting—suggest that the evolution of low-resistance vessel transport was a gradual process. Just as the anatomical distinction between tracheid and vessel can be quite subtle in basal angiosperms (Carlquist and Schneider 2002*a*), so might be the difference in conducting capability.

How did the evolution of vessels influence safety from cavitation by water stress? The "pit area hypothesis" (Wheeler et al. 2005; Hacke et al. 2006) suggests that the early stages of vessel evolution could have seriously increased the risk of cavitation. According to this hypothesis, the more area of interconduit pitting there is in a conduit, the greater the conduit's vulnerability to cavitation by air-seeding will be. This relationship was observed within our eudicot data set and also within vesselless angiosperms (Wheeler et al. 2005; Hacke et al. 2006, 2007). The causal explanation is that a greater total pit area increases by chance the size of the single largest pit membrane pore in a conduit. The single largest pore offers the weakest capillary barrier to air-seeding from embolized to functional conduits. If all of this is true, the evolution of multicellular vessels from unicellular tracheids should automatically bring with it a greater risk of cavitation because the total interconduit pit area will necessarily increase.

If the quantity of pits were all there were to it, however, all vessel-bearing species, whether basal or derived, would be more vulnerable to cavitation than vesselless species. This is not true. Our eudicot sample had an average cavitation pressure of −3.4 ± 0.4 MPa (Hacke et al. 2006), which is not different from the −3.4 ± 0.3 MPa average of the vesselless taxa (Hacke et al. 2007). The similar resistance to cavitation occurred despite the fact that the eudicot vessels averaged 56 times the interconduit pit area of vesselless species and so should be more vulnerable to cavitation by strict interpretation of the pit area hypothesis.

What we think has happened is a shift from large to small average pore size of interconduit pit membranes as vessels evolved from tracheids. A change in porosity is consistent with the greater intervessel pit resistance in eudicots compared with angiosperm tracheids and SEM observations of membranes (Hacke et al. 2007). The evolution of less porous membranes in concert with vessels makes adaptive sense. According to the pit area hypothesis, the less porous the membranes are on average, the more membrane area can be associated with the same maximum pore size per conduit. Evolving less porous pit membranes compensates for the increase in membrane area with greater conduit size, maintaining safety from cavitation by air-seeding.

The implication is that two opposing processes in pit membrane evolution were occurring in conjunction with vessel evolution. Some pit membranes were becoming more porous and evolving into scalariform perforation plates. Other pit membranes were becoming less porous and evolving into intervessel pits. The difficulty of achieving this delicate balance may have compromised safety from cavitation during early stages of vessel evolution.

We tested the hypotheses that vessel evolution decreased flow resistance but initially compromised safety from cavitation by measuring these properties on our sample of basal taxa (fig. 1; table 1). Thus, we used data from extant taxa to infer ancestral characteristics, an inevitable difficulty in evaluating evolutionary trends.

Material and Methods

Material and methods followed the protocol in the companion article on vesselless taxa (Hacke et al. 2007). To avoid repetition, details are provided in this article only when different methodology was required for studying vesseled wood.

Table 1

Species, Collection Locale, Habitat, Growth Form, and Parameters Not Shown in Figures

Family/species	Abbreviation	Region/elevation/lat., long.	Habitat/growth form	$F_P \pm SE$	$F_L \pm SE$
Austrobaileyaceae:					
Austrobaileya scandens C.T. White	ASC	Australia, northern Queensland/Main Coast Range/1040 m/16°33′22.0″S, 145°16′29.8″E	Broad-leaved tropical rain forest/liana	.026 ± .004	.93 ± .16
Calycanthaceae:					
Calycanthus floridus L.*	CFL	Southeastern United States, western North Carolina/1109 m/35°12′9.3″N, 82°14′32.7″W	Temperate deciduous forest/understory tree	.136 ± .014	.68 ± .07
Idiospermum australiense (Diels) S.T. Blake*	IAU	Cairns, Australia, northern Queensland/10 m/Flecker Botanical Garden	Native to lowland broad-leaved tropical rain forest/forest tree 20–30 m tall	.059 ± .008	.90 ± .10
Canellaceae:					
Canella winterana Gaertn.	CWI	Miami, Florida/10 m/Fairchild Botanical Garden	Native to coastal hammocks of West Indies/small tree	.026 ± .006	.98 ± .17
Chloranthaceae:					
Ascarina lucida Hook. f.	ALU	New Zealand, West Coast South Island near Hokitika/30 m/42°45′2.75″ S, 171°03′28.1″E	Warm temperate lowland forest/understory tree and forest edges	.090 ± .016	.81 ± .15
Ascarina rubricaulis Solms	ARU	New Caledonia, near Noumea, Mont Dzumac/900 m/22°01′47.1″S, 166°8′9.5″E	Tropical mountain cloud forest/small tree of forest edges, gaps	.038 ± .002	.83 ± .039
Ascarina solmsiana Schltr.	ASO	New Caledonia, near Noumea, Mt. Koghis slopes/530 m/22°10′39.6″S, 166°30′22.9″E	Tropical montane forest/understory tree	.049 ± .05	.81 ± .05
Hedyosmum goudotianum var. *goudotianum* Solms	HGO	Costa Rica, Puntarenas Province, near Monteverde/1820 m/10°19′8.3″N, 84°47′370.1″W	Tropical montane cloud forest/small tree	.065 ± .005	.74 ± .06
Hedyosmum mexicanum C. Cordem	HME	Costa Rica, Heredia Province, slopes of Volcan Barva/2500 m/10°0.7′48.4″N, 84°07′31.2″S	Tropical montane cloud forest/medium tree to 10+ m	.078 ± .011	.82 ± .13
Cunoniaceae:					
Weinmannia pinnata L.	WPI	Costa Rica, Puntarenas Province, Monteverde Cloud Forest Reserve/1640 m	Tropical montane cloud forest/understory tree	…	…
Eupomatiaceae:					
Eupomatia laurina R. Br.	ELA	Cairns, Australia, northern Queensland, Flecker Botanical Garden/10 m	Native to broad-leaved tropical rain forest/tall shrub of understory	.073 ± .006	.85 ± .07
Himantandraceae:					
Galbulimima baccata F.M. Bailey*	GBA	Australia, northern Queensland, Kuranda Range/300 m/16°49′11.0″S, 145°38′43.3″E	Broad-leaved tropical rain forest/canopy tree, saplings collected	.094 ± .010	.80 ± .05
Schisandraceae:					
Illicium anisatum L.	ILA	Japan, near Kyoto/Ohe Experimental Forest, 220 m	Temperate mixed deciduous/evergreen forest/small tree	.024 ± .003	.85 ± .06
Illicium floridanum J. Ellis	IFL	New Orleans, Louisiana/Taylor Feild's living collection	Native to moist areas in warm temperate deciduous forest/understory tree	.018 ± .002	.88 ± .06
Illicium parviflorum Michx. ex Vent.	IPA	Central Florida, Alexander Springs vicinity/15 m/29°04′40.9″N, 81°35′0.8″W	Moist areas in warm temperate temperate deciduous forest/small tree of understory and forest gaps	.017 ± .002	.90 ± .03
Schisandra glabra (Brickell) Rehder*	SGL	Southeastern United States, northeastern Georgia/275 m/34°40′24.4″N, 83°21′14.5″W	Moist deciduous bottomland forest/liana	.015 ± .002	.94 ± .10
Ticodendraceae:					
Ticodendron incognitum Gómez-Laur. and L.D. Gómez	TIN	Costa Rica, Puntarenas Province, near Monteverde/1450 m/10°18′46.9″N, 84°48′31.5″W	Tropical montane forest/canopy tree	…	…
Trimeniaceae:					
Trimenia moorei (Oliv.) Philipson	TMO	Australia, northern New South Wales, Forestland State Forest/1150 m/29°14′58.95″S 152°07′26.3″E	Tall moist eucalypt forest and rainforest/vine	.09 ± .10	.86 ± .06
Trimenia neocaledonica Baker f.	TNE	New Caledonia, Province Nord, Mt. Aoupinie/890 m/21°10′56.9″S, 165°17′32.6″E	Tropical montane cloud forest/subcanopy tree	.041 ± .004	.86 ± .07

Note. F_P = fraction of vessel wall area occupied by intervessel pits; F_L = length between vessel endwalls per length of vessel. Asterisked species have simple perforation plates.

Plant Material

Species, collecting locale, habitat, and growth form are listed in table 1. Species were selected to represent basal vessel-bearing taxa according to current hypotheses of evolutionary relationships (fig. 1). Species were also selected for their relatedness to vesselless lineages studied in the companion article (fig. 1, bold). Vessel morphology was taken into account by selecting basal species with both scalariform and simple perforation plate morphologies (table 1). Our methods are best suited for woody plants with extensive secondary xylem, limitations that excluded *Sarcandra* and *Chloranthus* of the Chloranthaceae. Two species were selected, not for their basal position but rather for their primitive vessel morphology (*Ticodendron incognitum*, *Weinmannia pinnata*), based on reports of many-barred scalariform perforation plates with pit membrane remnants (Carlquist 1991, 1992*a*). On these two species, we only conducted a subset of measurements, excluding vulnerability curves, vessel lengths, and pit areas. Difficulty of collection and extensive measurement time also limited sampling.

Thirteen of the 19 species were collected in their native habitats, often with the assistance of experts in the local flora (see "Acknowledgments"). Voucher specimens were filed in J. S. Sperry's collection. Four species were obtained from cultivation in their region of origin and under similar climatic and soil conditions (table 1).

Stems ca. 0.8–1.5 cm thick and ca. 20–100 cm long were cut from plants in the field, taking care to avoid unhealthy branches or ones with large side branches. Longer lengths were taken for lianescent species with longer vessels. Living stem sections were wrapped in plastic bags and express mailed or hand carried to J. S. Sperry's laboratory at the University of Utah.

Most parameters reported are species means from measurements of five to six stems per species. Minimum flow resistance (no reversible embolism) and anatomical parameters were measured on the same set of stems. An additional two sets of stems were required for vulnerability curves and vessel length measurements. Remaining material was used for SEM observations. Flow resistance, vulnerability, and vessel length were all measured as soon as possible after collection. Measurements were made generally within 2–3 wk of collection, except for one shipment held up by the USDA, which delayed measurement by nearly 4 wk. As explained for the vesselless species (Hacke et al. 2007), we observed no ill effects of storage time on the measurements.

Flow Resistance and Anatomy

Measurement protocol for the sapwood area-specific resistivity (R_{Xa}; see table 2 for symbol definitions and units) was the same described for vesselless species (Hacke et al. 2007). The only difference was that for species with longer vessels, we used stem lengths much longer than the standard 14.2 cm to minimize the number of open vessels running through the stem segment. A large number of open vessels results in an underestimation of the flow resistance because endwalls are excluded (Sperry et al. 2005). From vessel length measurements, we estimated that the number of open vessels was significant in only three species, ranging from 9.5% for *Trimenia neocaledonica* to 11.5% in *Idiospermum australiense* and 23% in *Austrobaileya scandens*. This suggests our flow resistances were underestimated for these species.

Table 2

Definition of Parameters, Symbols, and Units

Symbol	Definition	Units
A_P	Total area of interconduit pits per conduit	mm^2
D	Average conduit diameter of species, corresponds to R_L	μm
F_L	Length between vessel endwalls per total vessel length	...
F_P	Area of interconduit pits per vessel wall area	...
L	Average conduit length	mm
L^*	Conduit length predicted from eudicot L vs. D regression	mm
r_P	Flow resistance through pits on membrane area basis	MPa s m^{-1}
R_C	Conduit resistivity	MPa s m^{-4}
R_L	Lumen resistivity	MPa s m^{-4}
R_{Ca}	Resistivity of conduit on lumen area basis	MPa s m^{-2}
R_{La}	Resistivity of conduit lumen on lumen area basis	MPa s m^{-2}
R_{PPa}	Resistivity of conduit perforation plates on lumen area basis	MPa s m^{-2}
R_{Wa}	Resistivity of conduit endwall on lumen area basis	MPa s m^{-2}
R_{Xa}	Resistivity of xylem on sapwood area basis	MPa s m^{-2}

Note. $R_{Ca} = R_{La} + R_{Wa} + R_{PPa}$, according to equation (3). All parameters correspond to species means. Resistance is defined as the pressure difference per volume flow rate and is not standardized for length of the flow path. Resistivity is pressure gradient per volume flow rate and is standardized for length. Both resistance and resistivity can be expressed on a cross-sectional-area basis.

Mucilage exudation was a problem in some of the species, particularly the two *Hedyosmums* but to a lesser extent *Ascarina solmsiana*, *Ascarina lucida*, and *Trimenia moorei*. Mucilage was observed coming from the cut ends of these species, and it was sometimes associated with steep increases in resistivity as measured over the standard succession of six 10-s intervals (see Hacke et al. 2007). To minimize this problem, secretion from the bark was prevented by peeling it away before attaching the stems to the tubing apparatus. We also retrimmed the ends with a razor blade and wiped them clean immediately before attachment. With these precautions, time courses of resistivity were similar to species where no mucilage was observed.

To break down sapwood-specific resistivity into its anatomical components, we first multiplied it by the number of conduits per sapwood area to obtain the average conduit resistivity (R_C). This "hydraulically average" conduit will be biased toward the more conductive conduits, which are likely to be the wider ones.

The average lumen component of conduit resistivity (R_L) was calculated from lumen diameters according to the Hagen-Poiseuille equation (viscosities for all resistance measurements and calculations adjusted to 20°C). Care was taken to

distinguish intervessel contacts from scalariform perforation plates—the two appeared superficially quite similar in some species.

The average conduit lumen diameter (D) was chosen to correspond to the average R_L. Like the average conduit resistivity, this hydraulically weighted diameter is biased to the larger-sized conduits. The cross-sectional area of a lumen of diameter D (assumed circular) was multiplied by R_L and R_C to obtain the average resistivity on a lumen cross-sectional-area basis (R_{La}, R_{Ca}). All measurements were made on a stem basis, allowing $n = 6$ estimates of R_{Xa}, R_{Ca}, R_{La}, and D per species.

The $R_{Ca} - R_{La}$ difference gave us an estimate of the additional resistance afforded by perforation plates and endwalls, assuming that lumen, endwall, and perforation plate components add like resistances in series. For the four species with simple perforation plates (table 1, asterisks), we assumed all of the difference was in the endwall, termed the "endwall resistivity" ($R_{Ca} - R_{La} = R_{Wa}$). Although some species can show a mixture of scalariform and simple perforation plates, we saw no scalariform plates in our samples, even in *Schisandra glabra*, where at least some species in the genus are reported to have scalariform plates (Carlquist 1999). As fully explained elsewhere (Wheeler et al. 2005; Hacke et al. 2006), R_{Wa} can be expressed as a function of intervessel pit area (A_P), vessel length (L), and membrane area-specific pit resistance (r_P):

$$R_{Ca} - R_{La} = R_{Wa} = \frac{A_L 2 r_P}{A_P L F_L}, \quad (1)$$

where A_L is the cross-sectional area of the conduit lumen (corresponding to D). The F_L term converts total vessel length to the length between endwalls, which is assumed shorter by the length of one endwall. Endwalls were defined as the region of overlap between adjacent vessels. The length of one endwall was determined as half the length of a vessel that was in contact with one or more adjacent vessels (Wheeler et al. 2005).

All parameters in equation (1) were measured, except r_P, which was estimated by solving the equation. The A_P was determined from measurements of the intervessel pit-area-per-vessel surface area (F_P) and the vessel surface area estimated as a perfect cylinder,

$$A_P = \pi D L F_P. \quad (2)$$

Methods of estimating F_L and F_P are described in Wheeler et al. (2005) and Hacke et al. (2006), and the conduit length measurement is explained below. Sampling error for species means was determined directly for all parameters except r_P and A_P, which were calculated from mean values, and error was propagated accordingly.

For species with all scalariform perforation plates, the $R_{Ca} - R_{La}$ difference was assumed to be the sum of endwall resistivity (R_{Wa}) and perforation plate resistivity (R_{PPa}):

$$R_{Ca} - R_{La} = \frac{A_L 2 r_P}{A_P L F_L} + R_{PPa}, \quad (3)$$

where the first expression on the right side is R_{Wa} broken down into its components from equation (1). In this case, we could not solve for r_P because there are two unknowns, r_P and R_{PPa}. As explained in the "Results" section, we were able to estimate R_{Wa} for these species and thereby obtain an estimate of R_{PPa}.

Conduit Length

We determined conduit length using the silicone injection method described previously (Wheeler et al. 2005; Hacke et al. 2006). Five to six stems per species were flushed to remove reversible embolism and injected with a 10 : 1 silicone/hardener mix (RTV-141, Rhodia, Cranbury, NJ). A small amount of the fluorescent optical brightener (Uvitex, Ciba Specialty Chemicals, Tarrytown, NY) was dissolved in chloroform (1% w/w) and mixed into the silicone (1 drop g^{-1}) to allow the silicone to be detected in stem cross sections with fluorescence microscopy. Stems were injected overnight at 30–50 kPa pressure, and the silicone was allowed to harden further at room temperature for another day.

Stems were sectioned at exponentially longer intervals starting usually at 2 to 6 mm from the injection end and ending at anywhere from 15 to 50 cm, depending on the species. Counts of silicone-filled conduits per area were made at each distance and converted to conduit-length distributions using the single-parameter exponential decay function employed by Cohen and others (Cohen et al. 2003; Wheeler et al. 2005; Hacke et al. 2006). Although this function fits the data well for vessels, it can underestimate tracheid lengths. For tracheids, we think the more flexible Weibull function is best (Hacke et al. 2007). In future work, we will probably use the Weibull even for vessels, although the results are quite similar for most vessel-bearing species regardless of which two functions are used. Vessel length distributions are short skewed (Zimmermann and Jeje 1981), and we used the log-transformed mean to represent vessel length of a stem, as in all of our previous work. The grand mean of all stems per species was used for the species mean.

Cavitation Vulnerability Curves

Vulnerability curves indicate the loss of conductivity caused by progressively more negative xylem pressure. We used the centrifugal force method to generate these curves for each of six stems per species (Alder et al. 1997). Stems were flushed to remove reversible embolism and trimmed to 14.2 cm as required to fit in the custom centrifuge rotor. The mean cavitation pressure was calculated from each curve, and the mean of the six means was used to represent the vulnerability of the species to cavitation.

For some exceptionally vulnerable species, such as *Canella winterana* (fig. 7), or species with especially wide and long vessels, such as the liana *A. scandens*, we checked the centrifuge vulnerability curves with curves generated using an air-injection method (Sperry and Saliendra 1994). For this method, we used longer stem segments, between 20 and 25 cm, and inserted them through a double-ended pressure chamber. Stems were flushed to remove embolism, and the initial conductivity was measured. Air pressure was increased inside the chamber and held for 10 to 15 min before being gradually released and the conductivity remeasured. The process was repeated with progressively higher air pressure until the conductivity was negligible.

As in previous comparisons (Hacke et al. 2006), we found the air injection and centrifuge curves generally agreed, even for very vulnerable species with large vessels. Even when the curves disagreed statistically at some of the applied pressures

the general shape was similar. In these cases, the air-injection curve indicated a greater resistance to cavitation. When this was the case, as for *A. scandens*, we chose the air-injection curve to represent the species. In the other liana, *S. glabra*, we only used the air-injection method to save material. In all other species, including *C. winterana*, where the air-injection data was identical, we used the centrifuge results.

Scanning Electron Microscopy (SEM) Observations

Five species (*Illicium anisatum*, *Hedyosmum goudotianum*, *Ascarina rubricaulis*, *Trimenia neocaledonica*, *Eupomatia laurina*) were prepared for the SEM to observe scalariform perforation plates and vessel endwall pitting as described in Hacke et al. (2007). Wood surfaces to be observed were exposed by splitting (cracking) with a razor blade. They were coated with platinum by vacuum evaporation (JE-4, JEOL, Tokyo) and viewed with a field-emission scanning electron microscope (JSM-6301F, JEOL) at an accelerating voltage of 2.5 kV.

Results

Surprisingly, the sapwood-area resistivity (R_{Xa}) of basal taxa with vessels (group average 2400 ± 574 MPa s m^{-2}, mean ± SE) was not significantly lower than that for the vesselless species studied previously (group average 2500 ± 417 MPa s m^{-2}; Hacke et al. 2007). Similar resistivity occurred despite the much greater diameter of the vessels. The two more derived taxa with primitive perforation plate morphology (*Ticodendron incognitum*, *Weinmannia pinnata*) had similarly high sapwood resistivities (fig. 2*A*, *WPI*, *TIN*). Although mucilage obstruction could have inflated resistivities in a few cases, this was not an issue for most species, where no mucilage secretion was observed. Just as with vesselless species, the sapwood area resistivity did not decrease with conduit diameter in the basal vessel-bearing species (fig. 2*A*). These results contrast with eudicot vessels, all with simple perforation plates, which had very low sapwood area resistivity as a group (563 ± 64 MPa s m^{-2}) and showed a strong decline with increasing vessel diameter (fig. 2*A*; data from Hacke et al. 2006).

Contributing to the high sapwood resistivity was a generally lower density of vessels in basal taxa (including *T. incognitum*, *W. pinnata*) as compared with eudicots (fig. 3). When resistivities were expressed on a conduit lumen area basis (R_{Ca}), what we call "basal vessels" for shorthand did have lower resistivity (435 ± 104 MPa s m^{-2}) than angiosperm tracheids (906 ± 89 MPa s m^{-2}), but even so, they were still much higher than eudicots with simple perforation plates (91 ± 9 MPa s m^{-2}; fig. 2*B*). Just as for sapwood resistivity (R_{Xa}), the conduit resistivity (R_{Ca}) of basal vessels did not decline with vessel diameter (fig. 2*B*). As previously shown (Sperry et al. 2006), the conduit resistivity of eudicots with simple perforation plates declined with diameter to the second power, in concert with the second-power decline in lumen resistivity predicted by the Hagen-Poiseuille equation (fig. 2*B*, *HP* lumen resistivity line).

Interestingly, three of the four basal taxa with simple perforation plates also had much higher sapwood- and conduit-level resistivity than their eudicot simple-plated counterparts (fig. 2*A*, 2*B*). Only *Calycanthus floridus* (*CFL* in fig. 2*B*) fell in with the eudicot trend. The other three (*Idiospermum australiense*, *Schisandra glabra*, *Galbulimima baccata*) had much greater resistivity. Because we saw no scalariform perforation plates in these species, there must be another factor contributing to high resistivity in basal vessels.

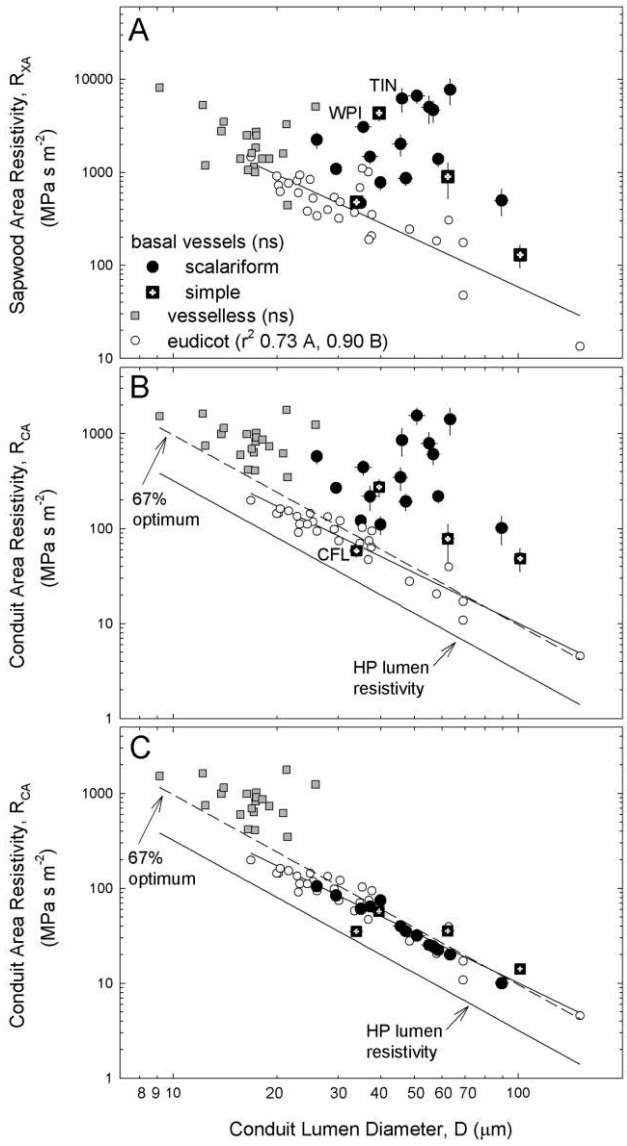

Fig. 2 Species averages for resistivity versus conduit diameter. Standard errors shown for basal taxa with vessels (table 1); simple- and scalariform-plated species distinguished by symbols. Vesselless angiosperm data are from the companion article (Hacke et al. 2007), and eudicot data are from Hacke et al. (2006). Individual species are labeled with abbreviations from table 1. Nonsignificant relationships lack regression lines. *A*, Resistivity on sapwood area basis (R_{Xa}). *B*, Resistivity on a lumen cross-sectional-area basis (conduit area resistivity, R_{Ca}). Solid line is lumen area resistivity (R_{La}) according to the Hagen-Poiseuille equation. Dashed line is for endwall resistivity (R_{Wa}) at 67% of total conduit resistivity. This optimizes conduit area resistivity for a fixed vessel length (Sperry et al. 2006). *C*, Same as *B* but with basal vessels adjusted for effects of short vessels and scalariform perforation plates. Subtracting these factors results in typical eudicot resistivities, suggesting they are responsible for the high resistivity of "primitive" vessels.

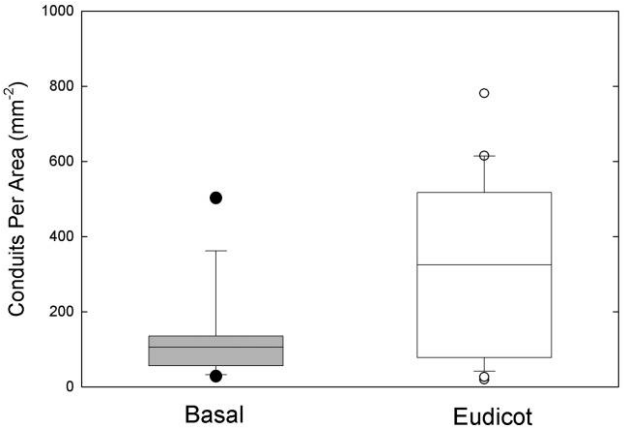

Fig. 3 Number of conduits per cross-sectional wood area for basal taxa (all taxa in table 1) and eudicot taxa (from Hacke et al. 2006). Boxes mark twenty-fifth to seventy-fifth percentile range, with the midline marking the median. Vertical lines show tenth to ninetieth percentile range, with outlying points as symbols. The grand means for species in the two wood types are significantly different.

The additional factor appears to be conduit length. Basal vessels of at least some taxa, including the simple-perforated species, tended to be short for their diameter compared with the eudicot sample (fig. 4). Other than the tendency to be short, vessel length in basal taxa increased similarly with diameter as eudicot vessel length.

The effect of short vessels is to increase the endwall resistivity (R_{Wa}; eq. [1]). For the simple-perforated species, where we were able to measure R_{Wa}, it averaged 81% of the total conduit resistivity (R_{Ca}). This is considerably greater than the 56% average in eudicots (Hacke et al. 2006). When we adjusted the R_{Ca} of basal vessels by increasing vessel length to the eudicot regression, it dropped to values within the eudicot range (fig. 2*C*). To make this calculation, we decreased R_{Wa} by the factor L^2/L^{*2}, where L^* is the length of a vessel based on the length versus diameter regression for the eudicot data (fig. 4) and L is the measured length. This "eudicot R_{Wa}" was added to the lumen resistivity (R_{La}), which is not influenced by length, to obtain the adjusted R_{Ca} value plotted in figure 2*C*. The L^2/L^{*2} factor was obtained by substituting equation (2) for A_P into equation (1) for R_{Wa}, which indicates R_{WA} is proportional to $1/L^2$.

For the species with scalariform perforation plates, the combination of endwall and perforation plate resistivity ($R_{Wa} + R_{PPa}$) accounted for 91% of the total conduit resistivity. We estimated (see next paragraph) that the scalariform perforation plate resistivity (R_{PPa}) accounted for 56% ± 16% of the total conduit resistivity, averaging 371 ± 131 MPa s m^{-2} (fig. 5, right bar). Endwalls accounted for 36% ± 16% of the conduit resistivity, with the balance in the lumen component. As a control, we made the same R_{PPa} estimate for simple-plated species (eudicots and the four basal taxa), which appropriately was not different from 0 (fig. 5, left bar).

We could not determine R_{PPa} directly because equation (3) has two unknowns: R_{Wa} and R_{PPa}. Instead, we made an independent estimate of R_{Wa} because in eudicots, it accounted for an average of 56% of the R_{Ca} regardless of vessel size (Hacke et al. 2006). This translates into $R_{Wa} = R_{La}/0.79$ (using eq. [1]). We used this relation to calculate R_{Wa} for the scalariform-plated species from their R_{La}. Adding the two ($R_{La} + R_{Wa}$) gives the conduit resistivity in the absence of any scalariform plates or deviation from the eudicot length-diameter scaling. These conduit resistivities closely match the eudicot regression line (fig. 2*C*). We then corrected this R_{Wa} for deviation from eudicot length-diameter scaling using the same L^2/L^{*2} conversion factor explained previously. The length-adjusted R_{Wa} was subtracted from the total measured conduit resistivity (R_{Ca}) to estimate the perforation plate resistivity (R_{PPa}). The R_{PPa} is not nearly as length sensitive as R_{Wa} because mean vessel element length varied much less between the species concerned (by a maximum factor of 2–3; Carlquist 1990, 1992*b*, 1992*d*, 1999; Carlquist and Schneider 2002*b*) than the vessel length (by as much as a factor of 20; fig. 3).

The potential for primitive scalariform plates to substantially increase flow resistance was obvious from SEM observations, which indicated substantial pit membrane remnants in many species. *Illicium anisatum* (fig. 6*A*), *Ascarina rubricaulis* (fig. 6*C*), *Hedyosmum goudotianum* (fig. 6*E*), and *Trimenia neocaledonica* (fig. 6*F*) all exhibited vestigial pit membranes of varying extent across the perforation plate openings. In general, they tended to be most dense at the periphery of individual openings (fig. 6*A*, 6*C*, 6*E*, 6*F*) and at openings toward either end of the scalariform plate (not shown). In some cases, there appeared to be discrete "perforations within a perforation," where the vestigial membrane gave way to large well-defined holes (e.g., *H. goudotianum*, *T. neocaledonica*; fig. 6*E*, 6*F*). In other cases, the membrane was more of a continuous open lacing of microfibrils (*I. anisatum*, *A. rubricaulis*; fig. 6*A*, 6*C*). Membrane remnants were not seen as frequently in *Eupomatia laurina*.

Twelve of the 17 basal study taxa (excluding *T. incognitum* and *W. pinnata*, which were not measured for cavitation) had xylem that was exceptionally vulnerable to cavitation

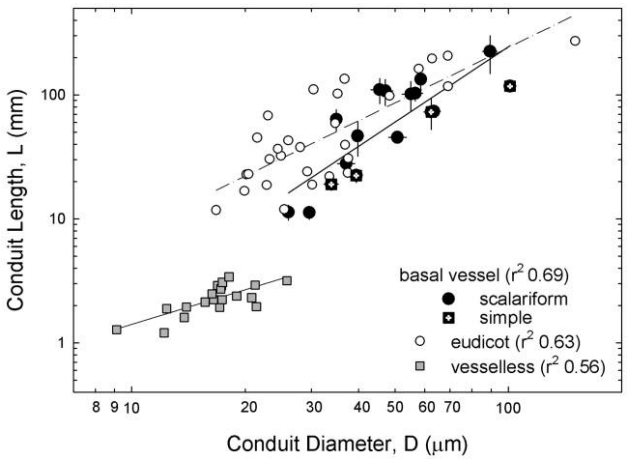

Fig. 4 Species averages for vessel or tracheid length and diameter. Standard errors shown for basal taxa with vessels (table 1); simple- and scalariform-plated species distinguished by symbols. Angiosperm tracheid data are from companion article (Hacke et al. 2007), and eudicot data are from Hacke et al. (2006).

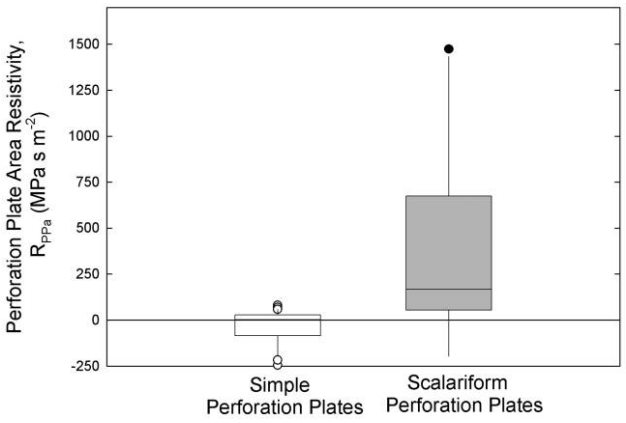

Fig. 5 Resistivity of scalariform perforation plates on lumen cross-sectional basis (R_{PPa}), estimated by assuming the same endwall versus lumen resistivity relationship as eudicot vessels and adjusting for deviations in length versus diameter scaling. As a control, an estimate no different from 0 was obtained for simple-perforation-plated species, including all eudicots (from Hacke et al. 2006) and the four simple-plated basal taxa (table 1, asterisked species). Box plot percentiles as indicated in fig. 3.

(fig. 7). The susceptible taxa had vulnerability curves with no cavitation threshold. Instead, there was measurable loss of conductivity beginning with the most modest negative pressure applied. Only the *Ascarina* and *Illicium* species had a threshold-type vulnerability curve typical of all the vesselless angiosperms (Hacke et al. 2007). As a group, the basal taxa had a less negative mean cavitation pressure (-2.0 ± 0.2 MPa) than either the vesselless species (-3.4 ± 0.3 MPa) or eudicots (-3.4 ± 0.4 MPa; fig. 8). These results support the hypothesis that there was a "vulnerability bottleneck" associated with initial stages of vessel evolution.

The relationship between pit area per conduit (A_P) and mean cavitation pressure was much noisier in basal vessels (fig. 9, $r^2 = 0.34$) than seen previously for eudicot vessels (fig. 9, $r^2 = 0.77$; Hacke et al. 2006) or vesselless angiosperms (fig. 9, $r^2 = 0.49$; Hacke et al. 2007). Twelve of the 17 species fell within the strong eudicot trend. Of the remaining five, two *Illicium* species (*I. anisatum*, *I. floridanum*) were indistinguishable from the vesselless data in having much less pit area per cavitation pressure than the eudicots (fig. 9, *IAN*, *IFL*). The other three species (*Trimenia moorei*, *Canella winterana*, *E. laurina*) also had less pit area per cavitation pressure but were much more vulnerable than the vesselless taxa (fig. 9, *TMO*, *CWI*, *ELA*). In the "Discussion" section, we consider how this variation in pit area per cavitation pressure relates to a shift toward less porous pit membranes during vessel evolution.

There was no evidence of a trade-off between protection from cavitation and xylem resistivity either on a sapwood or conduit basis (data not shown). Although species more resistant to cavitation tended to have narrower average vessel diameter ($r^2 = 0.38$; data not shown), this did not translate into greater flow resistance because there was no relationship between conduit size and flow resistance (fig. 2*A*, 2*B*).

Discussion

The most important result of our study was that the basal taxa with vessels did not conduct water more efficiently at the sapwood level than their vesselless relatives. Although basal vessels were marginally more efficient on a conduit cross-sectional-area basis than angiosperm tracheids, this did not propagate to the sapwood level because there are fewer vessels per wood area than tracheids. This result contradicts the hypothesis that the advantage of lower flow resistance drove the evolution of vessels from tracheids (Carlquist 1975; Zimmermann 1983; Bond 1989).

The surprisingly high resistivity of woods with "primitive" vessels relative to eudicot woods was associated with three variables: fewer vessels per sapwood area, a tendency for vessels to be shorter for their diameter, and the presence of long scalariform perforation plates with many bars and often with pit membrane remnants. Adjusting for these deviations from the eudicot pattern accounted for all of the increased resistivity in vessels of basal angiosperms. The results suggest that low resistivity did not evolve with vessels but only much later after adjustment of length, perforation plate morphology, and vessel frequency to the eudicot pattern (at least those eudicots with simple perforation plates). More extensive sampling of taxa that bridge the gap in phylogeny and vessel morphology between our basal and eudicot groups would further test this conclusion.

Our results suggested that primitive scalariform perforation plates were major obstructions to flow, accounting for 57% of the total flow resistivity on average. The resistivity of the plates themselves (R_{PPa}) averaged 371 MPa s m^{-2}, corresponding to an average of 35 times the lumen resistivity and 21 times the endwall resistivity. At first glance, it seems impossible to have a perforation plate resistivity that is greater than the endwall value because perforation plates evolved by opening up endwall pitting and reducing its flow resistance. The endwall, however, represents the overlap between contiguous vessels. The average length of the overlapping endwall spanned a distance (average 11 mm; data not shown) many times the length of a perforation plate (ca. 0.8–2 mm). The greater extent of the endwall can make its resistance per conduit length less than that of a perforation plate.

Our numbers for scalariform perforation plate resistivity are far greater than previous estimates. By a variety of different analyses, scalariform plate resistance was found to be from 0.6% to 50% of the vessel element resistance, which would be only 0.006 to 1 times the lumen resistivity (Petty 1978; Schulte et al. 1989; Schulte and Castle 1993*a*, 1993*b*; Ellerby and Ennos 1998). Scaled to a vessel 50 μm in diameter (average for our data set), this corresponds to an R_{PPa} of 0.08 to 12.8 MPa s m^{-2}, which is far below our average of 371 MPa s m^{-2}. Our figures are very crude estimates and exhibit high variation (fig. 5). They are also based on averaging across heterogenous xylem structure in a stem. A more direct measurement is preferable but difficult. Even so, a very high perforation plate resistivity is implied because the measured conduit resistivity in these species averaged nearly five times that of eudicot vessels with simple perforation plates (fig. 2*B*), and that discrepancy was not in every species associated with markedly shorter vessels (fig. 4) or any other obvious parameter.

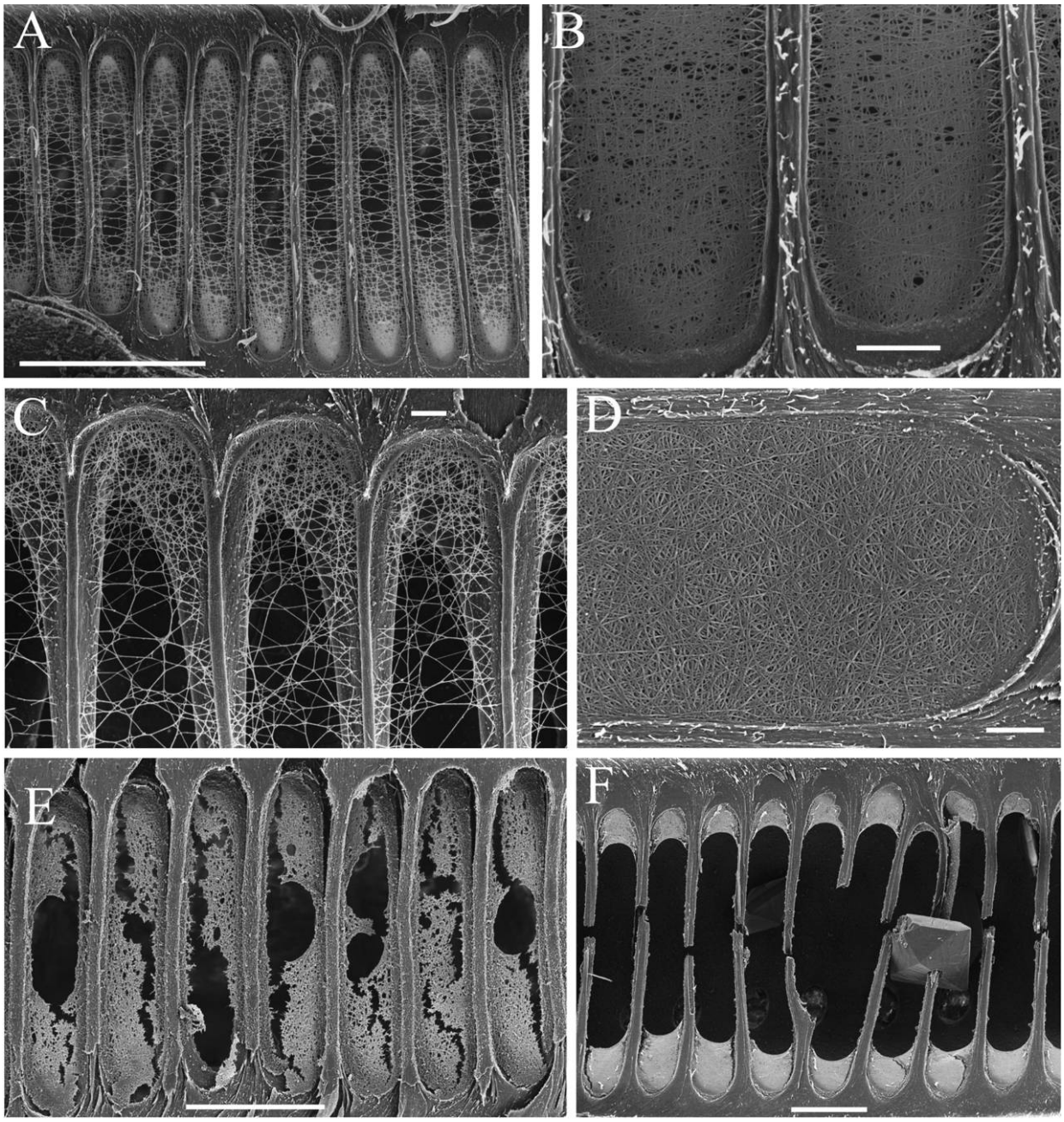

Fig. 6 SEM taken between 1600 (*F*) and 17,000 (*B*) magnification showing scalariform perforation plates (*A*, *C*, *E*, *F*) and intervessel pits (*B*, *D*). *A*, Scalariform perforation plate of *Illicium anisatum* showing extensive pit membrane remnants. Scale bar = 10 μm. *B*, Porous intervessel pit membrane of *I. anisatum*. Scale bar = 1 μm. *C*, Scalariform perforation plate of *Ascarina rubricaulis* laced with pit membrane remnants. Scale bar = 1 μm. *D*, Intervessel pit of *A. rubricaulis* showing much less porosity than in *I. anisatum* above. Scale bar = 1 μm. *E*, Perforation plate of *Hedyosmum goudotianum* with extensive pit membrane remnants (cracked) and also with large elliptical openings. Scale bar = 10 μm. *F*, Perforation plate of *Trimenia neocaledonica* with pit membrane remnants confined to the edges, suggesting large elliptical openings. Note crystal surrounding one bar. Scale bar = 10 μm.

Assuming our perforation plate estimates are at least approximately correct, there are good reasons they might be much greater than previous results. The most obvious reason is that previous estimates were for more "standard" perforation plate morphology typical of *Liriodendron* and *Betula* species with less than 30–40 bars (Petty 1978; Schulte and Castle 1993*a*). We were working with usually very primitive scalariform plate morphology, averaging well more than 50 bars in most species (to 134 in *Hedyosmum goudotianum*; Carlquist 1992*d*) and with the frequent presence of pit membrane remnants; features described by Carlquist in great detail for many of these species (Carlquist 1990, 1991, 1992*a*,

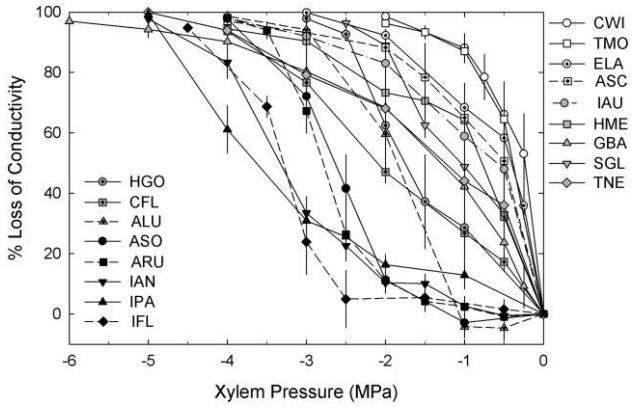

Fig. 7 Vulnerability curves of taxa in table 1 as abbreviated, except for derived taxa *Ticodendron incognitum* and *Weinmannia pinnata*. Curves show loss of xylem conductivity with increasingly negative xylem pressure. Means ± SE for six stems per species. Symbols are identified for most vulnerable (top right) to most resistant (left).

1992*d*; Carlquist and Schneider 2002*b*). Some previous estimates were also based on single-perforation plates in isolation (Schulte and Castle 1993*a*, 1993*b*; Ellerby and Ennos 1998), neglecting possible interactions between multiple plates spaced in series along the vessel.

Another reason is that scalariform perforation plate resistivity may be much more limiting in wider vessels. We found that the total conduit resistivity did not decrease with vessel diameter in the basal taxa. As a result, the discrepancy with eudicot vessels increased with vessel size (fig. 2*B*). This led to an increase in our R_{PPa} estimates for wider vessels (data not shown). If correct, this trend indicates that the cross-sectional area of the lumen increases more with lumen diameter than the decline in resistance per unit length through the perforation plate openings. There is reason to expect this because the width between the bars, and hence that component of their flow resistance, will not necessarily increase with lumen diameter. Furthermore, the length of the vessel elements typically decreases with increasing vessel diameter (Bailey and Tupper 1918), shortening the distance between perforation plates. These factors could increase the resistivity of the plate on a lumen cross-sectional basis in wider vessels.

Unfortunately, the previous studies of perforation plate resistance focused on plate angle and bar spacing for vessels of constant and relatively narrow diameter near the bottom of our range (e.g., 30–40 μm; Petty 1978; Schulte and Castle 1993*a*; Ellerby and Ennos 1998) and so did not assess the influence of wider vessel diameters. If our suspicion is correct, and scalariform plates are most disadvantageous in wide vessels, they should be selected against most strongly in wide-vesseled taxa. Perhaps this explains their very strong tendency to be most abundant in narrow-vesseled species generally (Baas 1986).

Our second most important result was the evidence for a "vulnerability bottleneck" in vessel evolution. There was no evidence that the increase in vulnerability going from vesselless to basal vessels was associated with a shift toward markedly wetter habitats for the vesseled species. The habitats of both species groups were all quite mesic, and in most cases, the vesselless and vesseled taxa were collected from the same locality, habitat, and climatic regime. Our interpretation is that this loss of safety from cavitation in basal vessels relative to the vesselless condition resulted from a functional constraint. To recapitulate the "Introduction," this constraint could be that the inevitable increase in pit area per conduit with vessel evolution leads to an inevitable increase in the single largest pit membrane pore per conduit and hence greater vulnerability to cavitation.

Acting to mitigate this constraint, we argue, was an approximately simultaneous shift from porous, low-resistance pit membranes between angiosperm tracheids to less porous, high-resistance pit membranes between evolving vessels. A change in membrane porosity is reflected in the jump from low conduit pit area per cavitation pressure in the angiosperm tracheid to much greater conduit pit area per cavitation pressure in the eudicot vessel (fig. 9, gray vs. open circles).

According to this interpretation, the noise in the pit area versus vulnerability relationship for basal vessels (fig. 9, solid circles) could represent intermediate stages in the evolution of low-porosity intervessel pits from high-porosity intertracheid pits. Hypothetically, the five species below the eudicot trend (fig. 9, *IAN*, *IFL*, *TMO*, *CWI*, *ELA*) have not completed the shift in membrane structure and have more porous membranes that are less resistant to flow than the 12 species on the eudicot line.

Two lines of evidence support this hypothesis. Our SEM observations indicate some heterogeneity in pit membrane porosity (cf. fig. 6*B*, 6*D*). Intervessel pits of *Illicium anisatum* (fig. 6*B*), a species below the eudicot line and matching the vesselless trend (fig. 9, *IAN*), included notably more porous membranes than those seen in the other species observed in the SEM that were on the eudicot line (e.g., fig. 6*D*, *Ascarina rubricaulis*).

A second, stronger line of evidence is that species that have less pit area than predicted from the eudicot regression also tend to have less pit area resistance (r_P) than the eudicot average (336 ± 81 MPa s m^{-1}) and vice versa (fig. 10, $r^2 = 0.65$). The less pit area per cavitation pressure a species exhibits, the

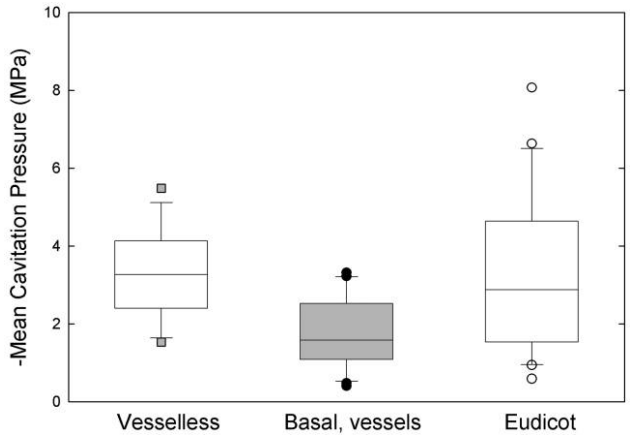

Fig. 8 Species mean cavitation pressures for basal taxa with vessels from fig. 7 compared with vesselless taxa from companion article (Hacke et al. 2007) and eudicot taxa from Hacke et al. (2006). Box plot percentiles for species mean values shown as in fig. 3.

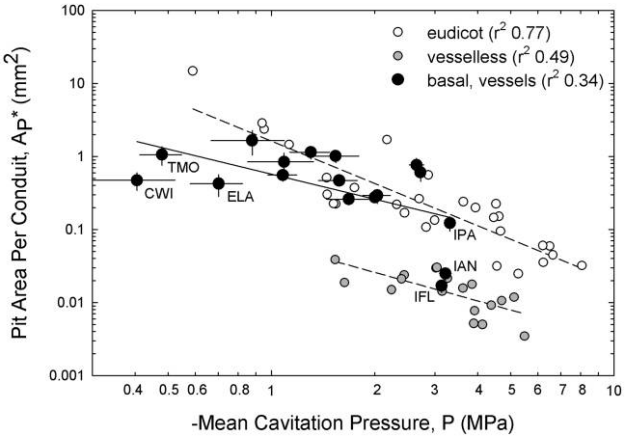

Fig. 9 Species means for interconduit pit area (A_P) and cavitation pressure. Standard errors shown for basal taxa with vessels (table 1, except derived *Ticodendron incognitum* and *Weinmannia pinnata*), some species identified by abbreviations in table 1. Vesselless angiosperm data are from the companion article (Hacke et al. 2007), and eudicot data are from Hacke et al. (2006).

lower is its pit area resistance and so the more porous on average are the pit membranes.

To summarize this hypothetical constraint, imagine that an ancestral tracheid had the same pit area per cavitation pressure relationship we found for vesselless angiosperms (fig. 9). The linking of tracheids into vessels would increase the pit area and move the evolving vessel inexorably along the same regression line to more modest cavitation pressure. Some vessels, like those of *I. anisatum* and *Illicium floridanum*, do not necessarily have more interconduit pit area than their antecedent tracheids because they are small enough and have low fractions of their walls as pits (F_P was only ca. 0.02 in these species; table 1). These two species also appear not to have adjusted their pit membrane porosity, falling as they do on the vesselless regression (fig. 9, *IAN*, *IFL*).

Most vessels, however, will have much greater interconduit pit areas. If they stayed on the same pit area/cavitation pressure regression as angiosperm tracheids, most would have cavitation pressures of essentially zero and be incapable of cohesion-tension–driven water transport (fig. 9). There would be tremendous selective pressure to adjust these intervessel pit membranes to lower average porosity and accommodate the increase in pit area without such a sacrifice in safety. Many of the basal species appear to have made this adjustment completely, others not at all (the *Illicium* pair), and some are at intermediate positions (*Trimenia moorei*, *Eupomatia laurina*, *Canella winterana*; fig. 9, *TMO*, *ELA*, *CWI*). Interestingly, the complete adjustment seems to have occurred even within a single genus, where *Illicium parviflorum* behaves like a eudicot while its congeners are indistinguishable from vesselless angiosperms (fig. 9, *IPA* vs. *IAN*, *IFL*).

It is intriguing to speculate that the proposed vulnerability bottleneck may be responsible for the curious concentration of aquatic and otherwise wet-adapted lineages at the base of the angiosperm tree. Nymphaeaceae, Ceratophyllaceae, Hydatellaceae, *Acorus*, and other basal monocots are all aquatic lineages that cluster near the base of the angiosperms. They are interspersed with the terrestrial, but very mesic adapted lineages that we sampled (Soltis and Soltis 2004; Saarela et al. 2007). Experiments with vessel evolution may have required very permissive environments to avoid extinction by cavitation.

Our two principal results pose an interesting question. If the early stages of vessel evolution resulted in no reduction in resistivity at the sapwood level and also resulted in a loss of safety from cavitation, why did angiosperm vessels evolve? We suggest that the advantage might not lie in vessels themselves but rather in the diversification of cell types in the secondary xylem made possible by vessel evolution. Our data do indicate that even primitive vessels were more efficient on a conduit basis than angiosperm tracheids (fig. 2*B*, lower R_{Ca} of basal vessels relative to tracheids). In this way, they could achieve the same sapwood resistivity but in less space, with the remaining space taken up with fibers and axial parenchyma systems.

To the extent this greater cell specialization conferred mechanical, storage, or other kinds of advantages relative to the homoxylous wood of vesselless angiosperms, it would be favored. Of course, this heteroxylous advantage would only be available in wet habitats, where the greater vulnerability of primitive vessels was not a problem (Feild et al. 2004).

A subtle, context-dependent advantage of primitive vessels relative to angiosperm tracheids is consistent with their phylogenetic relationship to vesselless taxa. Two prominent vesselless taxa, the Winteraceae and Trochodendrales, appear in a relatively derived position in the angiosperm tree (fig. 1; Soltis and Soltis 2004). Whether this resulted from reversion to vessellessness or multiple origins of vessels from persisting vesselless stock (Baas and Wheeler 1996), this phylogenetic pattern suggests that vessel evolution was not an immediate

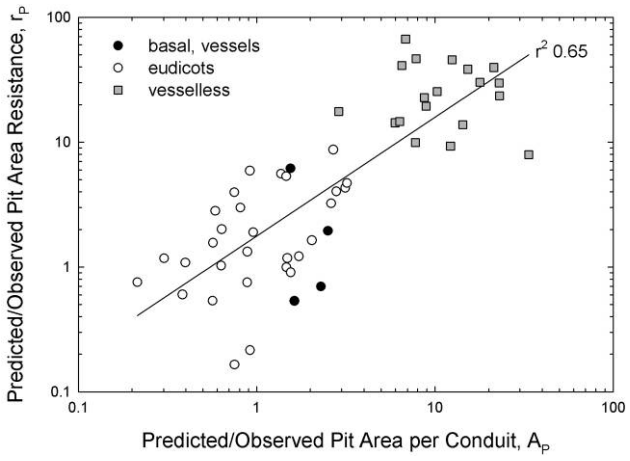

Fig. 10 Predicted/observed pit area resistance (r_P) versus predicted/observed pit area per conduit (A_P) for all species in fig. 9 except scalariform perforated ones, where r_P could not be determined. "Predicted" values correspond to eudicot average. In the case of pit area resistance, it was the average r_P for eudicot taxa (336 MPa s m^{-1}; Hacke et al. 2006) because r_P did not vary systematically with cavitation pressure. The "predicted" pit area corresponded to the eudicot regression for pit area versus cavitation pressure from fig. 9. The less pit area there was compared to the eudicot regression (moving right on the *X*-axis), the lower was the pit area resistance compared with the eudicot average (moving up on the *Y*-axis).

success story that rendered all other conducting systems obsolete. Only with the rise of the core eudicots and other diversifying lineages did vessel-bearing taxa radiate to dominance (Lupia et al. 1999). This delayed blooming is consistent with our functional data and inferences from structural data (Carlquist and Schneider 2002*a*) that suggests efficient and safe vessels took some time to evolve.

Inevitably, reconstructing evolution is speculative. But the diversity of xylem conduits that results from evolution is real, and it provides the opportunity for natural experiments in form and function. Our hypotheses of form-function linkages are imminently testable. In particular, more direct methods of estimating resistance components—pit, endwall, perforation plate—and different approaches to testing the pit area hypothesis are needed to evaluate our interpretation of how xylem structure influences flow resistance and cavitation vulnerability.

Acknowledgments

This work was funded by National Science Foundation grant IBN-0416297 to J. S. Sperry. Sabbatic leave to collect specimens was granted to J. S. Sperry by the University of Utah. In the early stages, Sherwin Carlquist provided useful advice on localities and taxon sampling. On-site experts aiding collection and identification were Stuart Worboys; Tony Bean (Australia); Phil Knightbridge (New Zealand); Gordon McPherson (New Caledonia); Takefumi Ikeda (Japan); Armando Soto, Barry Hammel, and William Haber (Costa Rica); Mary Collins (Fairchild Tropical Garden); and Kelly Bettinger (University of Georgia Herbarium). Y. Sano was supported by a grant-in-aid for scientific research (18580158) from the Ministry of Education, Culture, Sports, Science, and Technology, Japan.

Literature Cited

Alder NN, WT Pockman, JS Sperry, S Nuismer 1997 Use of centrifugal force in the study of xylem cavitation. J Exp Bot 48:665–674.

Baas P 1986 Ecological patterns of xylem anatomy. Pages 327–351 *in* T. J. Givnish, ed. On the economy of plant form and function. Cambridge, Cambridge University Press.

Baas P, EA Wheeler 1996 Parallelism and reversibility in xylem evolution: a review. IAWA J 17:351–364.

Bailey IW 1944 The development of vessels in angiosperms and its significance in morphological research. Am J Bot 31:421–428.

——— 1953 Evolution of the tracheary tissue of land plants. Am J Bot 40:4–8.

Bailey IW, WW Tupper 1918 Size variation in tracheary cells. I. A comparison between the secondary xylems of vascular cryptograms, gymnosperms, and angiosperms. Proc Am Acad Arts Sci Soc 54: 149–204.

Bond WJ 1989 The tortoise and the hare: ecology of angiosperm dominance and gymnosperm persistence. Biol J Linn Soc 36:227–249.

Carlquist S 1975 Ecological strategies of xylem evolution. University of California Press, Berkeley. 259 pp.

——— 1983 Wood anatomy of *Bubbia* (Winteraceae), with comments on origin of vessels in dicotyledons. Am J Bot 70:578–590.

——— 1987 Presence of vessels in wood of *Sarcandra* (Chloranthaceae); comments on vessel origins in angiosperms. Am J Bot 74: 1765–1771.

——— 1990 Wood anatomy of *Ascarina* (Chloranthaceae) and the tracheid-vessel element transition. Aliso 12:667–684.

——— 1991 Wood and bark anatomy of *Ticodendron*: comments on relationships. Ann Mo Bot Gard 78:96–104.

——— 1992*a* Pit membrane remnants in perforation plates of primitive dicotyledons and their significance. Am J Bot 79:660–672.

——— 1992*b* Vegetative anatomy and relationships of Eupomatiaceae. Bull Torrey Bot Club 119:167–180.

——— 1992*c* Wood anatomy and stem of Chloranthus: summary of wood anatomy of Chloranthaceae, with comments on relationships, vessellessness, and the origin of monocotyledons. IAWA (Int Assoc Wood Anat) Bull 13:3–16.

——— 1992*d* Wood anatomy of *Hedyosmum* (Chloranthaceae) and the tracheid-vessel element transition. Aliso 13:447–462.

——— 1999 Wood and bark anatomy of Schisandraceae: implications for phylogeny, habit, and vessel evolution. Aliso 18:45–55.

Carlquist S, EL Schneider 2002*a* The tracheid-vessel transition in angiosperms involves multiple independent features: cladistic consequences. Am J Bot 89:185–195.

——— 2002*b* Vessels of *Illicium* (Illiciaceae): range of pit membrane remnant presence in perforations and other vessel details. Int J Plant Sci 163:755–763.

Cohen S, JP Bennink, MT Tyree 2003 Air method measurements of apple vessel length distributions with improved apparatus and theory. J Exp Bot 54:1889–1897.

Ellerby DJ, AR Ennos 1998 Resistances to fluid flow of model xylem vessels with simple and scalariform perforation plates. J Exp Bot 49: 979–985.

Feild TS, NC Arens, JA Doyle, TE Dawson, MJ Donoghue 2004 Dark and disturbed: a new image of early angiosperm ecology. Paleobiology 30:82–107.

Feild TS, MA Zwieniecki, TJ Brodribb, T Jaffre, MJ Donoghue, NM Holbrook 2000 Structure and function of tracheary elements in *Amborella trichopoda*. Int J Plant Sci 161:705–712.

Frost FH 1930 Specialization in secondary xylem of angiosperms. I. Origin of vessel. Bot Gaz 89:67–92.

Hacke UG, JS Sperry, TS Feild, Y Sano, EH Sikkema, J Pittermann 2007 Water transport in vesseless angiosperms: conducting efficiency and cavitation safety. Int J Plant Sci 168:000–000.

Hacke UG, JS Sperry, JK Wheeler, L Castro 2006 Scaling of angiosperm xylem structure with safety and efficiency. Tree Physiol 26: 689–701.

Lupia R, S Lidgard, PR Crane 1999 Comparing palynological abundance and diversity: implications for biotic replacement during the Cretaceous angiosperm radiation. Paleobiology 25:305–340.

Petty JA 1978 Fluid flow through vessels of birch wood. J Exp Bot 29:1463–1469.

Saarela JM, HS Rai, JA Doyle, PK Endress, S Mathews, AD Marchant, BG Briggs, S Graham 2007 Hydatellaceae identified as a new branch near the base of the angiosperm phylogenetic tree. Nature 446: 312–315.

Schulte PJ, AL Castle 1993*a* Water flow through vessel perforation plates: a fluid mechanical approach. J Exp Bot 44:1135–1142.

——— 1993*b* Water flow through vessel perforation plates: the effects of plate angle and thickness for *Liriodendron tulipifera*. J Exp Bot 44:1143–1148.

Schulte PJ, AC Gibson, PS Nobel 1989 Water flow in vessels with simple or compound perforation plates. Ann Bot 64:171–178.

Soltis PS, DE Soltis 2004 The origin and early diversification of angiosperms. Am J Bot 91:1614–1626.

Sperry JS, UG Hacke, J Pittermann 2006 Size and function in conifer tracheids and angiosperm vessels. Am J Bot 93:1490–1500.

Sperry JS, UG Hacke, JK Wheeler 2005 Comparative analysis of end-wall resistance in xylem conduits. Plant Cell Environ 28:456–465.

Sperry JS, NZ Saliendra 1994 Intra- and inter-plant variation in xylem cavitation in *Betula occidentalis*. Plant Cell Environ 17:1233–1241.

Wheeler JK, JS Sperry, UG Hacke, N Hoang 2005 Inter-vessel pitting and cavitation in woody Rosaceae and other vesselled plants: a basis for a safety vs. efficiency trade-off in xylem transport. Plant Cell Environ 28:800–812.

Zimmermann MH 1983 Xylem structure and the ascent of sap. Springer series in wood science. Springer, Berlin. 143 pp.

Zimmermann MH, AA Jeje 1981 Vessel length distribution of some American woody plants. Can J Bot 59:1882–1892.